Palaeogeography, Palaeoclimatology, Palaeoecology 505 (2018) 287–294

Contents lists available at ScienceDirect

Palaeogeography, Palaeoclimatology, Palaeoecology

journal homepage: www.elsevier.com/locate/palaeo

Vegetation change and evolutionary response of large mammal fauna during the Mid-Pleistocene Transition in temperate northern East Asia

Zhou Xinying[a,c,d,*], Yang Jilong[b], Wang Shiqi[a,c,d], Xiao Guoqiao[e], Zhao Keliang[a,c,d], Zheng Yan[a,c], Shen Hui[a,c], Li Xiaoqiang[a,c,d]

[a] Key Laboratory of Vertebrate Evolution and Human Origins of Chinese Academy of Sciences, Institute of Vertebrate Paleontology and Paleoanthropology, Beijing 100044, China
[b] Tianjin Centre, China Geological Survey, Tianjin 300170, China
[c] University of Chinese Academy of Sciences, Beijing 100000, China
[d] CAS Center for Excellence in Life and Paleoenvironment, Beijing 100044, China
[e] State Key Laboratory of Biogeology and Environmental Geology, China University of Geosciences, Wuhan 430074, China

ARTICLE INFO

Keywords:
Pollen
Climate change
Co- evolution
Quaternary
Adaptation
Ecosystem

ABSTRACT

We present new pollen data from a drilling core from the North China Plain which illustrate the nature of vegetation evolution in the temperate zone of Asia during an interval containing the Mid-Pleistocene Transition (MPT), ~1.2–0.7 Ma. Results show that, from 1.7–1.2 Ma, closed needle-leaved and broadleaved mixed forest predominated. The most important vegetation change event occurred at 1.2 Ma when there was a decline in coniferous forest and a significant increase in *Artemisia*, Chenopodiaceae and Poaceae grassland. There was a continued degradation of the regional forest vegetation and its replacement by woody grassland about 0.7 Ma. Patterns of vegetation change correlate closely with the key climate fluctuations of the MPT and coincide with major turnover events of large mammalian fauna (> 10 kg) in China. In particular, > 50% of large mammalian species became extinct in the course of the forest decline; however, they were replaced by new mammalian species after 0.7 Ma. Comparison of the vegetation and faunal records indicates that the process of forest replacement by grassland in the northern temperate zone during the MPT was associated with an acceleration of the rate of turnover of the large mammalian fauna, in terms of extinction and speciation.

1. Introduction

During the late Cenozoic, the global climate underwent major changes including an ongoing temperature decrease and initiation of the polar ice caps (Liu and Ding, 1993; Zubakov and Borenkova, 1990). The Mid-Pleistocene climatic transition (MPT) (1.2–0.7 Ma) is one of the most important intervals of climate change during the late Cenozoic and is sometimes also called the Mid-Pleistocene revolution (Clark et al., 2006; Lisiecki and Raymo, 2005). Since 1.2 Ma, a significant increase in global ice volume occurred periodically, which generally began in MIS 36, accompanied by an increase in the amplitude of the climate variability (Polyak et al., 2010; White et al., 2010). The intensity of the Asian winter monsoon increased significantly and the climate of the interior of Eurasia became significantly colder (Polyak et al., 2010; White et al., 2010). During the interval of 1.2–0.7 Ma, the relatively low-amplitude 41-kyr obliquity-forced climate cycles of the earlier Pleistocene were progressively replaced by high-amplitude 100-kyr cycles (Lisiecki and Raymo, 2005). Thus there was a major change in the mode of climatic variability from a pattern of high frequency, low amplitude fluctuations in the early Pleistocene to a pattern of low frequency and high amplitude fluctuations in the later Pleistocene (Head and Gibbard, 2005).

The onset of a phase of global cooling and ice expansion during the middle Pleistocene likely caused a major restructuring of the global vegetation and faunal systems, and the nature of the co-evolution of plants, animals and the global climate system during the MPT is of significant interest (e.g., Alroy et al., 2016; Harington, 2008;Norton et al., 2010;Gaboardi et al., 2005; Potts, 2012; Bobe and Behrensmeyer, 2004; Behrensmeyer et al., 1997). One finding is that there was a significant adaptation of the mammalian fauna in response to the changing global or regional climate and environment (Alroy et al., 2016; Norton et al., 2010). Moreover, it has been suggested that climate and environmental change was an important factor in determining or influencing the course of mammalian faunas and lineages at this time

* Corresponding author at: Key Laboratory of Vertebrate Evolution and Human Origins of Chinese Academy of Sciences, Institute of Vertebrate Paleontology and Paleoanthropology, Beijing 100044, China.
E-mail address: zhouxinying@ivpp.ac.cn (X. Zhou).

https://doi.org/10.1016/j.palaeo.2018.06.007
Received 4 February 2018; Received in revised form 31 May 2018; Accepted 3 June 2018
Available online 06 June 2018
0031-0182/ © 2018 Elsevier B.V. All rights reserved.

(Lister, 2011).

The response of terrestrial vegetation in the northern temperate zone to the MPT is important for understanding the nature of the co-evolution of plants, animals and the Pleistocene climatic system (Norton et al., 2010; Deng et al., 2002). Because the northern temperate zone is located on the margin of the Northern Hemisphere ice sheets which existed during glacial maxima, its vegetation is likely to have exhibited a high degree of sensitivity to the glacial advances and retreats. Moreover, the northern temperate zone is also the core area of the glacial megafauna evolution (Lister, 2011).

Important questions include what was the response of the vegetation change in the north temperate zone to the new pattern of climatic variability associated with the MPT, and how did the mammalian fauna adapt to the regional vegetation change? In order to address these questions, here we present a new pollen data from a drilling core from the North China Plain that sheds light on the pattern of vegetation change in the temperate northern East Asia. In addition, we integrate our findings with published fossil mammal data to assess the co-evolution of plants, animals and global climate during the MPT.

2. Regional physiographic setting

The North China Plain (Fig. 1, 32°–40°N, 114°–121°E) is located on the northeastern margin of the Chinese mainland close to the Bohai Bay. It is the largest alluvial plain in North China, and has an average elevation of 50 m and was formed from the deposits of the Yellow River, Haihe River and Huaihe River. The regional climate belongs to the typical warm temperate monsoon zone. The annual average temperature is 8–15 °C and the rainfall gradually decreases from 800 mm in the south (the Huaihe River area) to 500 mm in the north (the Haihe River Area). > 50% of the rainfall of the area is associated with the Asian summer monsoon and thus is mainly distributed in the summer. Thus, there are distinct seasonal changes with winter and autumn being cold and dry, the spring hot and dry, and the summer hot and humid.

The modern vegetation of the North China Plain is mainly temperate shrub-grassland dominated by chaste tree (*Vitex negundo*), jujube (*Ziziphus jujube*) and bluestem (*Bothriochloa ischaemum*), and themeda (*Themeda japonica*). The higher elevation areas are occupied by warm temperate deciduous broadleaved and needle-leaved mixed forest (Chinese Academy of Sciences, 2001). The dominant broadleaved species include *Quercus acutissima* and *Quercus variabilis* in the south, and *Quercus mongolica* and *Quercus liaotungensis* in the north. The needle-leaved trees are dominated by *Pinus*, mainly *Pinus densiflora*. Other common northern temperate species, including *Betula costata*, *Eleutherococcus senticosus*, *Juglans mandshurica* and *Tilia*, are also present. The proportion of shrub-grassland dominated by Gramineae, *Artemisia*, Rosaceae, *Betula Salix*, *Ulmus* increases gradually from south to north (Chinese Academy of Sciences, 2001). In addition, wetland vegetation is widely distributed in the northern part of the plain, consisting typically of *Phragmites*, *Typha*, *Scirpus* and *Carex*, with saltmarsh dominated by Chenopodiaceae on the coast (Chinese Academy of Sciences, 2001).

The Bohai Basin represents the youngest land-sea transition in East Asia and was characterized by significant changes in climate, distribution of fresh water and sediment fluxes (Hu et al., 2001; Qi and

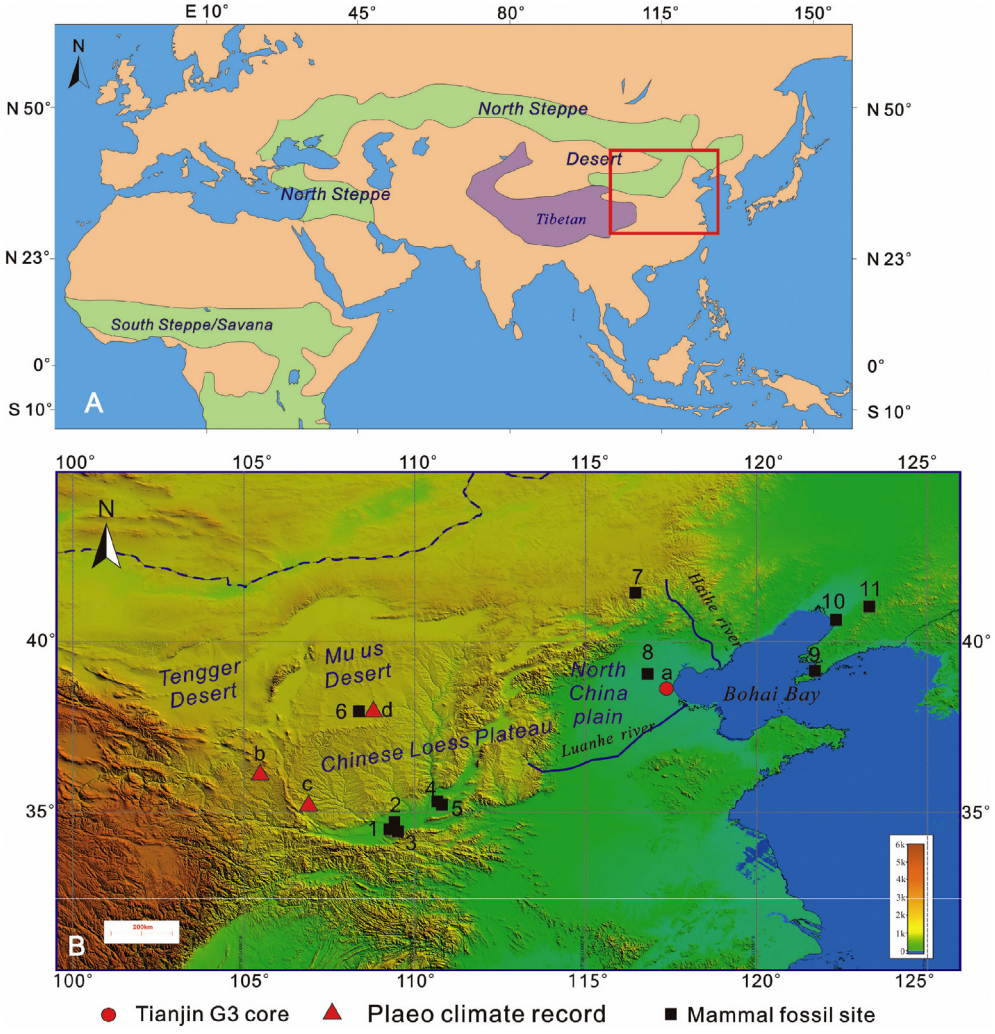

Fig. 1. A: Location of the study area in Eurasia and grassland vegetation zones, red box is represented by B. B: Location of the Tianjin-G3 core in the North China Plain and climate records and fossil mammal sites mentioned in the text. a. Tianjin G3 core (this study), b. Duanjian section (Yang et al., 2006), c. Caona section (Wu et al., 2007), d. Jingbian section (Ding et al., 2005), 1. Gongwangling, 2. Yangguo, 3. ChenJiawo, 4. Xi Houdu, 5. Kehe, 6. Sjara-osso-gol, 7. Nihewan, 8. Zhoukoudian, 9. Gulongshan, 10. Jinniushan, 11. Miaohoushan. the map and vegetation data in A and B is from http://www.webmap.cn/, the DEM data in B is from ftp://edcftp.cr.usgs.gov. (For interpretation of the references to color in this figure legend, the reader is referred to the web version of this article.)

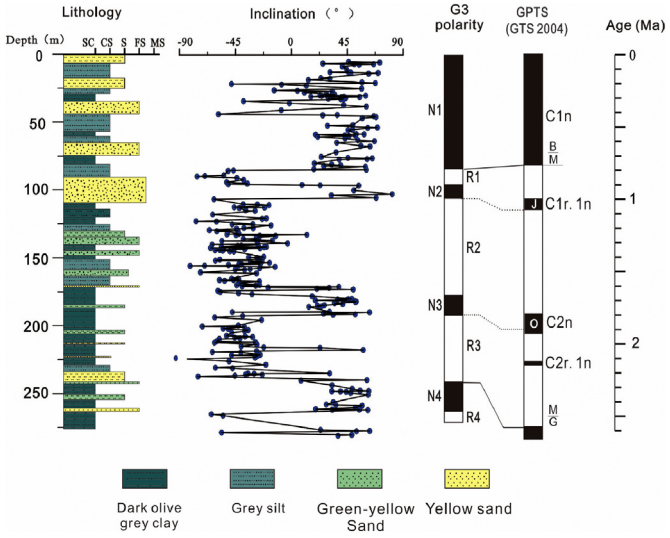

Fig. 2. Lithology and magnetostratigraphy of Tianjin-G3 core (Depth 0–275 m) and comparison with GTS 2004 (Gradstein et al., 2005); Lithology grain size classification: sandy clay (SC), clayey sand (CS), sand (S), fine sand (FS), medium sand (MS).

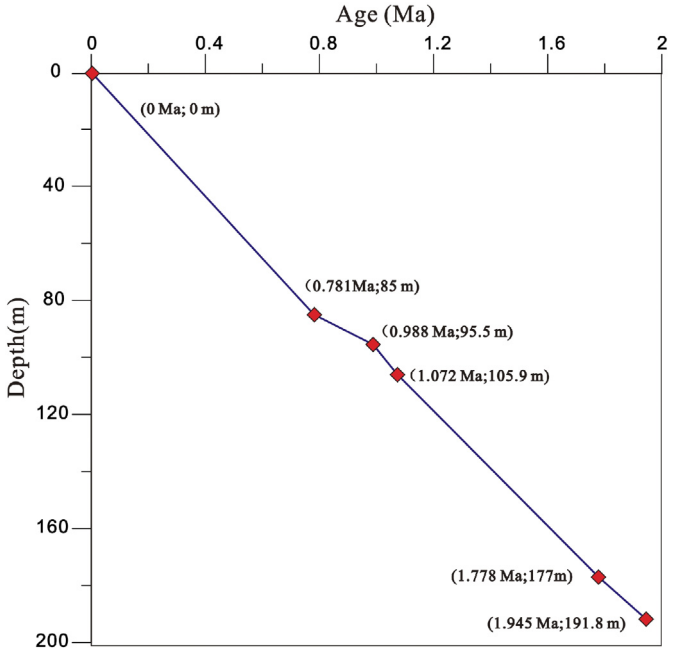

Fig. 3. Age-depth relationship for core Tianjin-G3, based magnetostratigraphy.

Yang, 2010). The Bohai Paleolake originated in the late Pliocene and terminated around the late Middle Pleistocene; the land bridge separating the Bohai basin and the Pacific Ocean disappeared only by 0.3–0.1 Ma, resulting in the subsequent maturation of the basin as an inner shelf sea (Yi et al., 2016).

3. Materials and methods

3.1. Lithology and magnetostratigraphy

Sediment core Tianjin-G3 (117°25′59.5″N, 38°49′57.6″E) was drilled in the eastern part of the North China Plain, close to Bohai Bay. The core is 250 m in depth and the recovery ratio is 90.0%, which meets the requirements for magnetostratigraphic study. The lithology consists of alluvial and lacustrine facies with varying amounts of clay, silt, and silty sand. Typical marine facies are present at depth of 5.0–18 m, representing a marine transgression from 8000 to 5000 cal yr BP, which is widely represented in east China (Xiao et al., 2014).

The lithology, paleomagnetic inclination and inferred polarity stratigraphy of Tianjin G3 and its correlation with the geomagnetic polarity timescale are illustrated in Fig. 2. Five geomagnetic polarity intervals are recognized, including three normal polarity intervals, N1 (0–85.0 m), N2 (95.5–105.9 m) and N3 (177–191.8 m); and two reversed polarity intervals, R1 (85.0–95.5 m) and R2 (105.9–177.0 m). N1 is correlated with the Brunhes normal polarity chron (C1n, 0–0.781 Ma). R1–R3 are correlated with the Matuyama reversed polarity chron epoch, among which N2 (95.5–105.9 m) is correlated with the Jaramillo polarity subchron (C1r.1n, 0.988–1.072 Ma) and N3 (177–191.8 m) with the Olduvai normal polarity subchron (C2n, 1.778–1.945 Ma) (Yang et al., 2016). For reference the Olduvai subchron has been reported in previous published magnetostratigraphic studies undertaken near Bohai Bay (Xiao et al., 2014; Yang et al., 2016). N4 is correlated with the upper part of the Gauss normal polarity chron (c2an.1n). The resulting age-depth relationship of the core is shown in Fig. 3.

3.2. Pollen analysis

Pollen samples were collected from the interval 0–250 m depth of the Tianjin-G3 core. 100 g of sediment was used for pollen analysis at each sample interval and pretreatment consisted of the following stages: 1) Addition of hydrochloric acid to remove carbonates; 2) flotation with 2.0 s-class heavy liquid flotation (with $ZnCl_2$ and KI-ZnI_2); 3) addition of a 1:9 solution of concentrated sulfuric acid and acetic anhydride; 4) suspension in glycerol and mounting on microscope slides. At least three pollen slides were produced and checked for each sample. Pollen counting was conducted with an OLYMPUS biological photomicroscope at ×400 magnification. Fossil pollen grains were identified via comparison with published photomicrographs and modern pollen reference slides. The total pollen count exceeded 150 grains in most samples (mean 167 grains per sample). The samples below 170 m failed to yield sufficient pollen grains for analysis. A pollen diagram for the interval from 0 to 170 m (0–1.73 Ma) was produced using Tilia 2.0.

Detrended Correspondence Analysis (DCA) has proven to be highly successful for hypothesis generation with paleoecological data (Clark, 1986; Bush et al., 1990). DCA axes represent hypothetical environmental gradients that explain major variance in the pollen data set. DCA is not unduly influenced by slight variations in the percentage occurrence of the major taxa, and as the percentage occurrence of the major taxa, and as the percentage occurrence of the most abundant taxa tend to stabilized at a count of 200 pollen. When pollen count are insufficient, pollen taxa will also decrease correspondingly, and the results reflected by DCA will be somewhat biased, but it is still an important reference to judge past vegetation changes. The DCA analysis of this study was performed using CANOCO 4.5.

4. Results

We analyzed a total of 80 samples among which 61 samples had a high pollen concentration. Pollen was abundant in the 61 samples collected from above 170 m. A total of 9167 pollen grains consisting of 48 genera and species were counted and identified. The coniferous tree pollen types include *Tsuga*, *Abies*, *Picea*, and *Pinus*; and the broadleaf tree types include *Quercus*, *Betula*, *Carpinus*, *Alnus*, *Castanea*, *Tilia*, *Juglans*, *Ulmus*, *Aphananthe*, *Liquidanber*, *Carya* *Corylus* and Sapindaceae. The shrub pollen types include Acanthaceae, Elaeagnaceae, *Ostryopsis*, *Ephedra* and Rosaceae. The herb pollen types include *Artemisia*, Chenopodiaceae, Compositae, Gramineae, *Sanguisorba*, *Humulus*, Rubiaceae, Labiatae, Leguminosae, Solanaceae, *Polygonum*, Cruciferae, Caryophllaceae and Umbelliferae. Aquatic

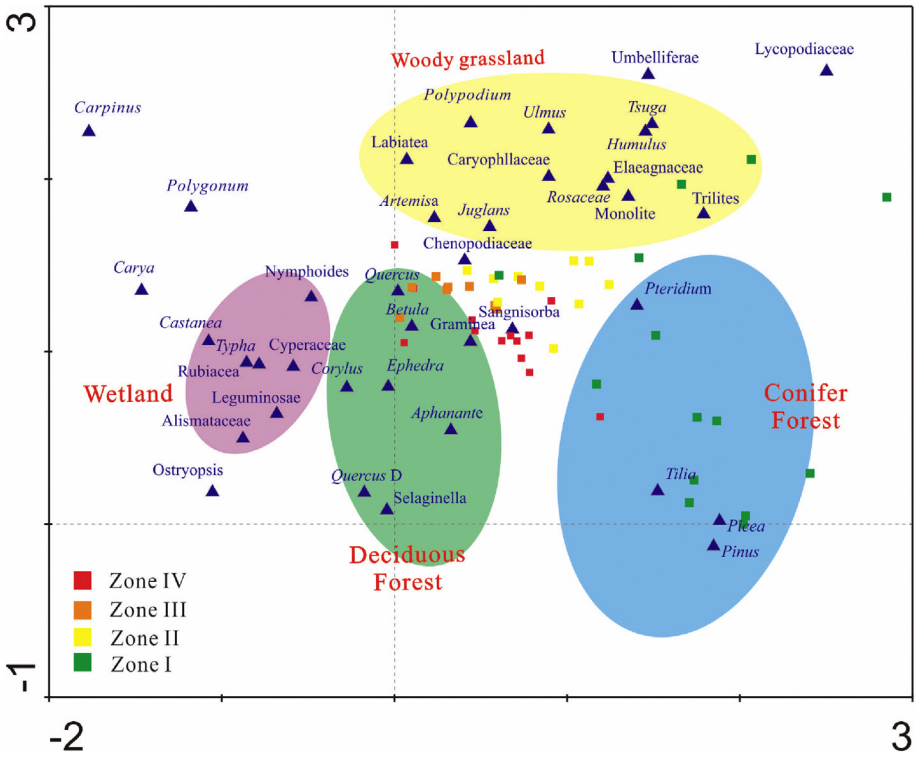

Fig. 4. Results of Detrended Corespondence Analysis (DCA) of the pollen data in Tianjin-G3 core generated by CANOCO 4.5. Eigenvalues: Axes 1 = 0.386, Axes 2 = 0.202, blue triangles represent species, color squares represent samples from different pollen zone. (For interpretation of the references to color in this figure legend, the reader is referred to the web version of this article.)

pollen types include Alismataceae, *Typha*, Cyperaceae and *Nymphoides*; and fern spore types include Lycopodiaceae, *Polypodium*, *Pteridium*, *Selaginella*, Parkeriaceae, Monolites and Trilites.

Detrended correspondence analysis (DCA) of the pollen data was conducted using CANOCO 4.5 and a plot of the distributions of the pollen taxa and samples on the first two axes is illustrated in Fig. 4. The DCA show that the first two axes have eigenvalues of 0.386 and 0.202, respectively, which explains 58.8% of the species data. According to the modern taxa distribution as mentioned above, the pollen taxa distributions can be divided into four main groups: 1) Temperate coniferous forest taxa, principally *Picea* and *Pinus*. 2) Deciduous broadleaf forest taxa; e.g., *Quercus*, *Betula* and *Corylus*. 3) Wetland taxa; e.g., *Typha*, Alismataceae, *Nymphoides* and Cyperacea. 4) Woody grassland taxa; e.g., *Ulmus*, Rosaceae, *Artemisia*, Chenopodiaceae, *Humulus* etc. The distributions of the stratigraphic samples have also been illustrated in the DCA biplot, to show the vegetation type represented by the pollen data from each zone as the following description.

The percentage pollen diagram for Tianjin-G3 is illustrated in Fig. 5. Also shown are the results of stratigraphically-constrained cluster analysis implemented using CONISS software. In addition to considering the results of the CONISS analysis of G3 pollen data, the zoning of the pollen diagram pay more attention on changes in the major representative plant taxa such as *Pinus*, *Quercus*, *Betula*, *Artemisia*, Rosaceae, and Chenopodiaceae, which take higher proportion in the pollen assemblage and with clear environmental directive. The pollen diagram can be divided into four main pollen assemblage zones, which are described below.

4.1. Pollen Assemblage Zone I (Pinus-Picea-Chenopodiaceae-Compositae-Ferns) (1.7–1.2 Ma)

The tree pollen frequencies average 58.6% and mainly include *Pinus* and *Picea*. During the early part of the zone the tree pollen taxa include *Tsuga*, and in the later part *Picea* at relatively high frequencies. Broadleaved tree taxa such as *Quercus*, *Betula*, *Juglans* and *Ulmus* are present at low frequencies. Chenopodiaceae is the main herb pollen type with an average of 8.1%. Other herb taxa include Compositae and *Artemisia*.

Zone I is indicative of a warm and humid temperate or subtropical needle-leafed and broadleaved mixed forest. *Pinus* was probably a dominant species, although it is typically over-represented in pollen diagrams. A significant change occurred at 1.55 Ma when *Tsuga* disappeared and was replaced by *Picea*. Compositae, which represents humid grassland, also decreased, and Chenopodiaceae and Poaceae increased. These changes indicate that the local climate gradually become drier and colder during this interval.

4.2. Pollen Assemblage Zone II (Quercus-Pinus-Betula-Chenopodiaceae–Artemisia) (1.2–0.7 Ma)

Pinus decreases from Zone I to this zone and *Picea* and *Tsuga* almost disappear. The representation of broadleaved trees such as *Quercus* and *Betula* increases significantly, and other tree pollen types appear, e.g., *Castanea*, *Ulmus*, and *Juglans*. There are also significant changes in herb taxa, with large increases in Chenopodiaceae, *Artemisia* and Poaceae. *Artemisia* exhibits the largest increase. In addition, *Typha* appears, with frequencies of ~5%.

Zone II is indicative of a mixture of warm temperate broadleaved forest and woody-grassland. The increase in herb pollen percentages, especially *Artemisia*, probably reflects an expansion of drought-tolerant woody grassland and shrinking of the area of forest.

4.3. Pollen Assemblage Zone III (Chenopodiaceae-Artemisia-Typha-Quercus-Betula (0.7–0.3 Ma)

Tree pollen frequencies reach their lowest level. *Pinus* and *Quercus* decrease, together with *Picea*, *Tsuga*, *Liquidambar* and *Carya;* however, *Betula* increases. *Artemisia* and Chenopodiaceae exhibit high frequencies. These characteristics indicate a continued expansion of temperate shrub grassland and shrinking of the forest. In the same time, the increase in *Typha* and Cyperaceae suggests an expansion of wetland in the region. This may be related to changes in the local topography and hydrological Environment. But the decrease in annual average temperature, due to the expansion of the northern hemisphere ice cap,

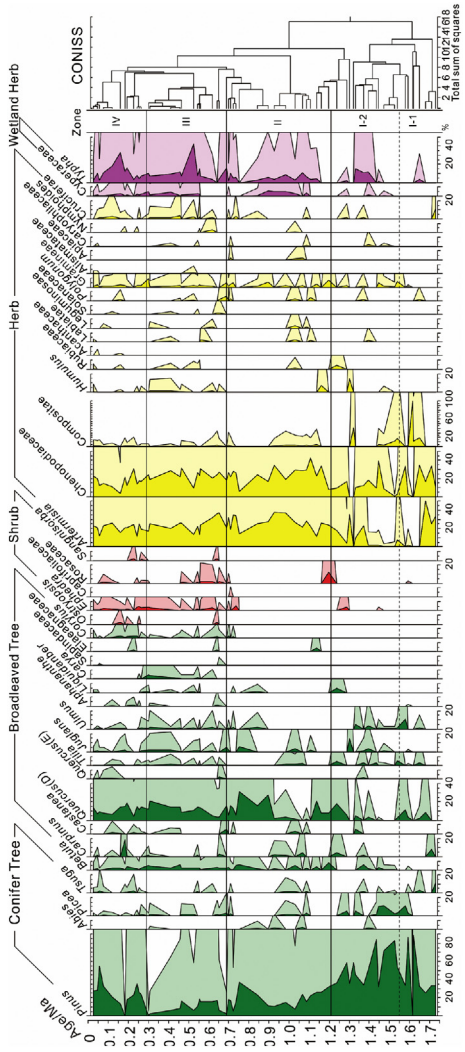

Fig. 5. Percentage pollen diagram and results of CONISS analysis for core Tianjin-G3.

could reduce the annual evaporation, which may also lead to an increase in regional wetlands. In summary, the pollen assemblages indicate woody-grassland vegetation with widely distributed lake and wetland environments.

4.4. Pollen Assemblage Zone IV (Chenopodiaceae–Artemisia-Typha-Pinus-Quercus) (0.3–0 Ma)

Pinus increases on average, and there are also increases in *Picea* and *Tsuga*. In addition, *Quercus* decreases and *Liquidambar* and *Carya* disappear and *Tilia*, *Castanea*, *Ulmus* and *Juglans* are present at low frequencies. There is a decrease in Chenopodiaceae and an increase in *Typha*. This zone indicates a warm coniferous-broadleaved mixed forest with woody-grassland, and an increase in the extent of wetland.

5. Discussion

5.1. Response of the vegetation of the north temperate zone to the Mid-Pleistocene Transition

During the MPT, paleoclimatic records from mid- and high- latitudes of the Northern Hemisphere, such as from deep-sea sediment cores and terrestrial loess sections, indicate a change in the character of the climatic response to earth orbital forcing from low amplitude, high frequency to high amplitude, low frequency variability (Clark et al., 2006). Specifically, there was a shift in the pattern of variation of northern hemisphere ice volume from predominantly 41-kyr tilt forcing, affecting low latitude heat distribution, to 100-kyr forcing by orbital centricity. This transition was initiated at about 1.2 Ma or 1.0 Ma, and proceeded gradually and was completed after about 0.7–0.6 Ma (Lisiecki and Raymo, 2005; Wang et al., 2003). During the transition, average global ice volume increased by about 15% with large increases at high and middle latitudes of Eurasia and North America during glacial maxima (Hughes et al., 2010; Kauman and Manley, 2004; Marjanac and Marjanac, 2016). Earth orbital variations (Milankovitch forcing), via their effects on summer isolation at mid-latitudes of the northern hemisphere, are strongly imprinted on the ice volume variations (Clark et al., 2006), although the origin of the shift from the dominant mode of variability from 100-kyr to 41-kyr variability is debated.

The pollen record of the Tianjin-G3 core from the North China Plain reveals significant changes in vegetation composition during the MPT (1.2–0.7 Ma). The coniferous - deciduous broadleaved mixed forest, dominated by *Quercus* and *Pinus*, shrank significantly, with the proportion of forest in the local vegetation decreasing further after 0.7 Ma. The representation of ferns, indicative of a moist environment, began to decrease at around 1.2 Ma and they were much less abundant after 0.7 Ma. By contrast, *Artemisia* and Chenopodiaceae, representative of the grassland of temperate Eurasia, became prevalent after 1.2 Ma, and the local forest vegetation was transformed to grass-dominated grassland by around 0.7 Ma. In addition, *Betula*, a dominant tree in the northern cold temperate zone, became strongly represented in the pollen spectra at 1.2 Ma.

These changes indicate that from 1.2–0.7 Ma the coniferous and deciduous broadleaved mixed forest in the study area was transformed into sparsely-wooded grassland, and thus became part of the northern hemisphere grassland (Fig. 4). Similarly, the pollen record form the Chinese Loess Plateau also indicates a shrinkage of the area of woodland and an expansion of grassland (Fig. 6) (Wu et al., 2007). In addition, grain-size data from loess sections near the Mu Us and Tengger deserts indicate the commencement of a stepwise expansion at about 1.2 Ma, and that the process of aridification was further intensified after 0.7 Ma (Fig. 6) (Ding et al., 2005; Yang et al., 2006). These coherent large-scale regional changes indicate that the climate of the north temperate zone of China became significantly drier and that there was a degradation of woodland and expansion of grassland and desert (Fig. 6).

The best explanation for these large-scale environmental changes is that the MPT was associated with a decrease in temperature in both northern and southern hemisphere, and that the expansion of northern hemisphere ice sheets resulted in a weakening of ocean circulation and the global monsoon system. This resulted in decreased rainfall in much of the interior of the landmasses in both hemispheres. It is noteworthy that at around 1.6–1.5 Ma in the study area, thermophilous *Tsuga* was replaced by cold-tolerant *Picea*, which probably indicates that temperature had already begun to decrease before the onset of the climatic transition at 1.2 Ma.

5.2. Turnover of large mammalian fauna to the changes in climate and environment

The dynamics of the evolutionary response of both humans and mammals to environmental change during the glacial-interglacial ages of Quaternary has long been debated (Dennell et al., 2011; Harington, 2008). Natural selection, the process by which new adaptive structures evolve and persist, is viewed as the primary mechanism by which organisms change in relation to their environment. Long term shifts in climate and secular shifts in climate variability are two separate ecological signals which can establish natural selection opportunities (Demenocal, 2004). However the abundant evidence attests to

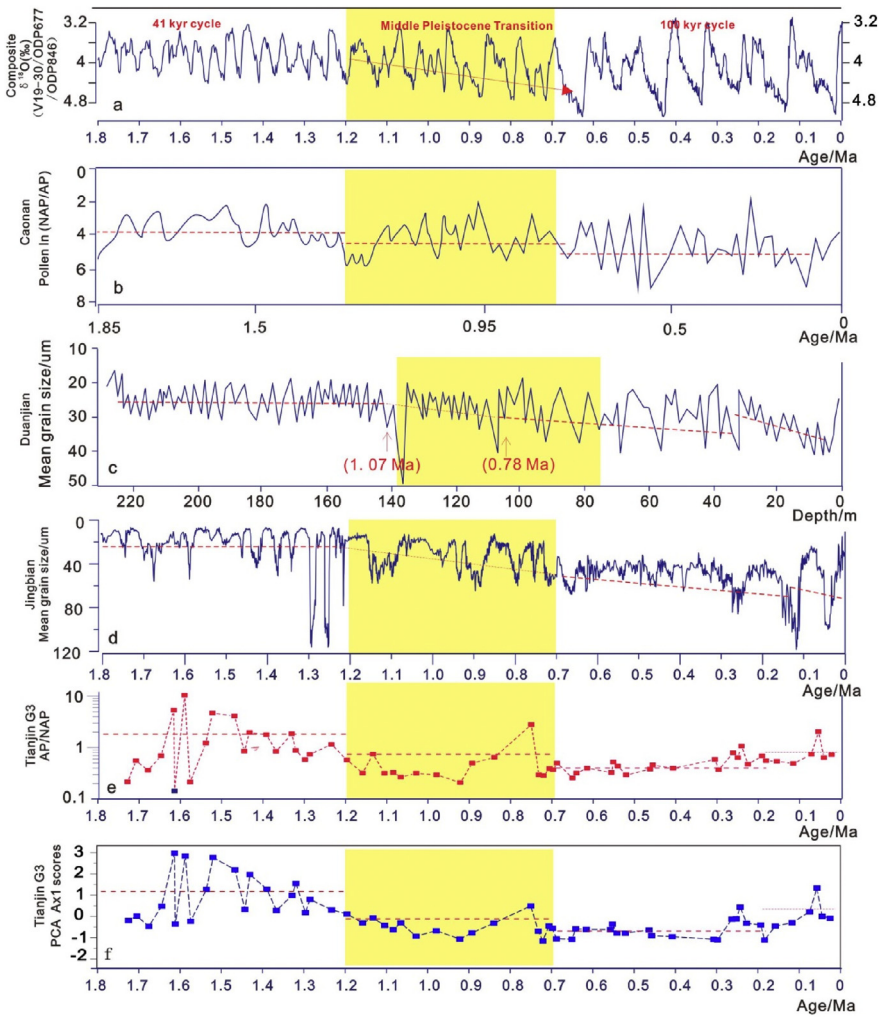

Fig. 6. Comparison of various paleoclimatic records spanning the MPT. (a) LR04 benthic $\delta^{18}O$ stack based on the graphic correlation of 57 globally-distributed benthic $\delta^{18}O$ records (Lisiecki and Raymo, 2005), (b) Ratio of arboreal pollen/non-arboreal pollen (AP/NAP) in the Caonan section in the Chinese Loess Plateau (CLP) (Wu et al., 2007). (c) Stepwise expansion of the Tengger desert indicated by the mean grain-size of the Duanjian section, western CLP (Yang et al., 2006). (d) Stepwise expansion of the Mu Us desert indicated by the mean grain-size record of the Jingbian section, northern CLP (Ding et al., 2005). (d) AP/NAP record from core Tianjin-G3 (this study). (e) AX1 scores from core Tianjin-G3. Yellow shaded interval is the MPT. (For interpretation of the references to color in this figure legend, the reader is referred to the web version of this article.)

population-level changes within the Quaternary, these did not usually lead to the origin of new species (Barnosky, 2005). It is clear that while a single glacial-interglacial cycle is too short to produce a new lineage, the rate of mammalian evolution increased significantly during the Pleistocene as a whole (Lister, 2011). Thus longer time scale climate transition, such as MPT, should be considered as the main climate factor influencing the mammalian evolution.

The impact of climate and environment changes on mammal evolution is comprehensive that include abiotic and biotic aspects. Firstly, abiotic factors, such as temperature, precipitation could be important factor affecting the faunal distribution and evolution (Smith et al., 2010). The morphological differences exhibited by the species of the same genus in different latitudes are significantly affected by the temperature gradient. And the seasonality change may cause the transform of adaptation strategy of mammal species. For example, large-scale herbivorous animal communities are often formed in the grassland of grassland area and migrate along with the seasons change (Fryxell and Sinclair, 1988). Secondly, biotic aspects changes, such as vegetational assemblages, related to climate variation could cause the regional faunal turnover. Forest ecologies provide multiple botanical foods like leaves, barks, nut and fruits that are relatively easy to chew and digest, while grassland ecologies are relatively single, mainly include stems, leaves of grass containing hard fabric and silicon that is hard to chew and digest (Shipley, 1999). Therefore, the appearances of high-crown grazing species in regional faunal were linked to aridity and expanding grasslands, and that normally together with regional decrease and extinct of low-crown teeth taxa (Kaiser et al., 2013). The carnivorous communities also have to adapt to climate changes and the changes of herbivore communities.

As mentioned earlier, the vegetation of temperate East Asian monsoon region may fluctuated along with the 40-ka cycle of the climate during the early to mid-Pleistocene period, but the region is covered by coniferous and broad-leaved mixed forests in most time. After MPT, the forests of the region quickly decreased, and shrub grasslands became dominated in most of the periods. These exhibited that the temperate vegetation in East Asia period have generally significant degraded during and after the MTP.

Comparison of the vegetation and mammalian fauna of the northern temperate zone during the Mid-Pleistocene reveals that there was a rapid and significant response of the mammalian fauna to the associated environmental changes (Fig. 7). Specifically, the expansion of woody-grassland during the MPT was associated with a rapid restructuring of the regional mammalian faunas in the North China Plain (Qiu, 2006).

The total number of large mammalian species decreased substantially during 1.2–0.7 Ma. Elements of the herbivorous faunas of the early and middle Pleistocene (2.0–1.2 Ma), found in Nihewan (Wei, 2004), Yangguo (Ji, 1975), Xihoudu (Wei, 2004), Zhoukoudian Loc.18 (Teilhard de Chardin, 1940), Gongwangling (Hu and Qi, 1978), including e.g. *Leptobas stenometopon* and *Hesperotherium* sp., became extinct in North China during 1.4–1.2 Ma, synchronous with the onset of the expansion of grassland. Key members of the grassland mammalian fauna, e.g. *Equus sanmenniensis*, *Sus lydekkeri*, *Paracamelus gigas* and *Cervus grayi*, remained the principal species during the transition. Most

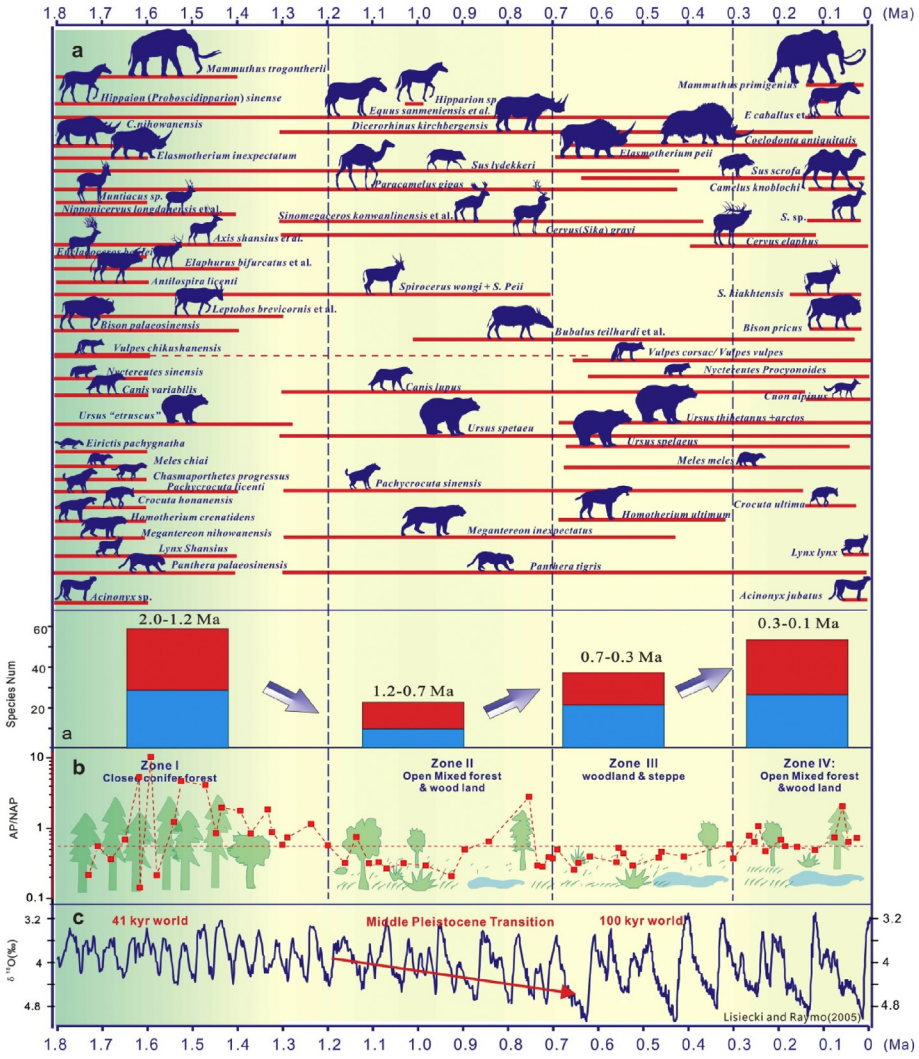

Fig. 7. Correlation of the vegetation history of the North China Plain with the pattern of mammalian evolution in North China, and global climate change since 1.8 Ma. (a) Temporal distribution of selected major representatives of the Quaternary mammalian faunas in North China (Qiu, 2006). (b), Species number change of selected large mammal in carnivores (in red bar) and herbivores (in blue bar). (c) Vegetation history of the North China Plain based on the pollen analytical results from core Tianjin-G3 (this study). (d) LR04 benthic $\delta^{18}O$ stack (Lisiecki and Raymo, 2005). (For interpretation of the references to color in this figure legend, the reader is referred to the web version of this article.)

of the carnivores of the early Pleistocene, e.g. *Megantereon* and *Homotherium*, did not survive the MPT, while new carnivorous species, including *Canis lupus*, *Ursus spetaeu*, *Pachycrocuta sinensis*, *Megantereon inecpectatus* and *Panthera tigris*, appeared at Kehe (Qiu et al., 1987), Zhoukoudian Loc.1 (Shen et al., 2009; Teilhard de Chardin and Pei, 1941) and Chenjiawo (Chow and Li, 1965) at around 1.2–0.7 Ma. Thus, the major expansion of grassland and decline of woodland, beginning at ~1.2 Ma BP, was accompanied by the coevolution of mammals adapted to grazing and open habitats.

By the end of the MPT, at 0.7 Ma, despite the continued expansion of grassland, there was a recovery in the total number of species comprising the mammalian faunas. The discovery in Jinniushan (Zhang, 1993), Miaohoushan (Museum of Liaoning Province and Museum of Benxi City, 1986), Salawusu (Sjara-osso-gol) (Wu et al., 1989) show that most of the members of the herbivorous faunas present from 1.2–0.7 Ma remained during 0.7–0.3 Ma. New species of the genera *Coelodonta* and *Elasmotherium*, which became extinct in the northern temperate area during 1.2–0.7 Ma, reappeared at the sites of Gulongshan, Jinniushan, Miaohoushan and Salawusu (Sjara-osso-gol). At the same time, carnivorous mammals such as *Vulpes*, *Nyctereutes*, *Meles* and *Homotherium*, also reappeared. Furthermore, members of the genera *Mammuthus*, *Bison*, *Crocuta*, *Lynx* and *Acinonyx* also reappeared during the late Pleistocene. Besides that, non-human primates, such as macaques, appeared in the Palearctic region probably in the end of the MPT at places like Zhoukoudian Locality 1 and sites of Korea (Norton, 2000; Jablonski et al., 2000), besides the fact that macaques made it to the Japanese archipelago probably in the same time (Norton, 2000). Considering that after 0.7 Ma the vegetation did not recover its former forest status, and that the colder and drier area of grassland continued to expand, the recovery of the regional mammalian faunas can only be explained in terms of their adaptation to the regional environmental changes. This process may be explained by the fact that due to the expansion of the Northern Hemisphere's ice cap during MPT, the winter temperature in Asia's mid-latitudes dropped significantly, and the forest vegetation shrank caused by the weakening of the Asia summer monsoon. The original grazing species remain in the region during this process, while some forest species became extinct, and some migrated to lower latitudes. It appears that the evolution of a new mammalian lineage that was adapted to the cooler drier grassland environment occurred over several hundred thousand years, and that the evolution rate was related to the characteristics of specific genera. The relatively high rate of mammalian evolution during the Pleistocene may have been mainly the result of the rapidity of the cooling trend and the vegetation transition rather than the glacial-interglacial cycles.

6. Conclusions

Pollen data from the Tianjin-G3 core from the temperate North China Plain indicate that the process of vegetation evolution from 1.7 Ma can be divided into four main stages: 1) 1.7–1.2 Ma, closed needle-leaved and broadleaved mixed forest; 2) 1.2–0.7 Ma, open warm temperate deciduous broadleaved forest; 3) 0.7–0.3 Ma, sparse forest-

grassland; 4) 0.3–0 Ma, open warm temperate deciduous broadleaved forest. Overall, the results reveal a decline in hygrophilous coniferous forest and expansion of the area of Chenopodiaceae- *Artemisia*-Gramineae-dominated grassland during the middle Pleistocene.

There is a clear relationship between the vegetation degradation in the North China Plain and the process of aridification of the Loess Plateau area. This indicates that the widespread aridification of the North Temperate Zone China was synchronous with stepwise climate change during the middle Pleistocene transition at about 1.2 Ma and then 0.7 Ma.

The climatic and related vegetation changes in north temperate China associated with the Mid-Pleistocene Transition (MPT) had a major effect on the composition of the large mammalian faunas. More than one half of the early Pleistocene species did not survive through the middle Pleistocene. However, subsequent to the MPT several members of the mammalian fauna were able to adapt to the new climatic and environmental conditions. Overall, our findings indicate large mammals had a strong ability to adapt to the changed conditions, but nonetheless the evolution of new species required hundreds of thousands of years.

Acknowledgments

We thank the National Natural Science Foundation of China (grants 41371003, 41572161) and the National Basic Research Program (grant 2015CB953800), and the Youth Innovation Promotion Association of Chinese Academy of Sciences (KC216403) for their financial support. We are also grateful to Xu Qinmian, Hu Yunzhuang, Qin Yafei, Li Jing for their assistance with the fieldwork. We thank Dr. Jan Bloemendal, Prof. Howard Falcon-Lang for polishing the text and the anonymous reviewers for their helpful suggestions.

References

Alroy, J., Koch, P.L., Zachos, J.C., 2016. Global climate change and North American mammalian evolution. Paleobiology 26, 259–288.
Barnosky, A.D., 2005. Effects of Quaternary climatic change on speciation in mammals. J. Mamm. Evol. 12, 247–264.
Behrensmeyer, A.K., Todd, N.E., Potts, R., et al., 1997. Late Pliocene faunal turnover in the Turkana Basin, Kenya and Ethiopia. Science 278 (5343), 1589–1594.
Bobe, R., Behrensmeyer, A.K., 2004. The expansion of grassland ecosystems in Africa in relation to mammalian evolution and the origin of the genus Homo. Palaeogeogr. Palaeoclimatol. Palaeoecol. 207 (3–4), 399–420.
Bush, M.B., Colinvaux, P.A., Wiemann, M.C., Piperno, D.R., Liu, K.-B., 1990. Late Pleistocene temperature depression and vegetation change in Ecuadorian Amazonia. Quat. Res. 34, 330–345.
Chinese Academy of Sciences, 2001. Vegetation Atlas of China (1:100000). Science Press, Beijing.
Chow, M.C., Li, C.K., 1965. Mammalian fossils in association with the mandible of Lantian Man at Chen Chia-ou. In: Lantian, Shensi. 9. Vert PalAsiat, pp. 377–393 (in Chinese with English summary).
Clark, J.S., 1986. Dynamism in the barrier-beach vegetation of Great South Beach, New York. Ecol. Monogr. 56, 97–126.
Clark, P.U., Archer, D., Pollard, D., Blum, J.D., Rial, J.A., Brovkin, V., Mix, A.C., Pisias, N.G., Roy, M., 2006. The middle Pleistocene transition: characteristics, mechanisms, and implications for long-term changes in atmospheric pCO_2. Quat. Sci. Rev. 25, 3150–3184.
Demenocal, P.B., 2004. African climate change and faunal evolution during the Pliocene–Pleistocene. Earth Planet. Sci. Lett. 220, 3–24.
Deng, T., Dong, J.S., Wang, Y., 2002. Variation of terrestrial ecosystem recorded by stable carbon isotopes of fossils in northern China during the Quaternary. Chin. Sci. Bull. 47, 76–78.
Dennell, R.W., Martinón-Torres, M., Castro, J.M.B.D., 2011. Hominin variability, climatic instability and population demography in Middle Pleistocene Europe. Quat. Sci. Rev. 30, 1511–1524.
Ding, Z.L., Derbyshire, E., Yang, S.L., Sun, J.M., Liu, T.S., 2005. Stepwise expansion of desert environment across northern China in the past 3.5 Ma and implications for monsoon evolution. Earth Planet. Sci. Lett. 237, 45–55.
Fryxell, J.M., Sinclair, A.R.E., 1988. Causes and consequences of migration by large herbivores. Trends Ecol. Evol. 3, 237–241.
Gaboardi, M., Deng, T., Wang, Y., 2005. Middle Pleistocene climate and habitat change at Zhoukoudian, China, from the carbon and oxygen isotopic record from herbivore tooth enamel. Quat. Res. 63, 329–338.
Gradstein, F.M., Ogg, J.G., Smith, A.G., 2005. A Geologic Time Scale 2004. Cambridge University Press.
Harington, C.R., 2008. The evolution of Arctic marine mammals. Ecol. Appl. 18, S23.
Head, M.J., Gibbard, P.L., 2005. Early-middle pleistocene transitions: an overview and recommendation for the defining boundary. J. Geol. Soc. Lond. 247 (1), 1–18.
Hu, C.K., Qi, T., 1978. Gongwangling Pleistocene mammalian fauna of Lantian, Shaanxi. Acta Palaeontol. Sin. New Ser. C 21, 1–64 (in Chinese with English Summary).
Hu, S., O'Sullivan, P.B., Raza, A., Kohn, B.P., 2001. Thermal history and tectonic subsidence of the Bohai Basin, northern China: a Cenozoic rifted and local pull-apart basin. Phys. Earth Planet. Inter. 126, 221–235.
Hughes, P.D., Woodward, J.C., Calsteren, P.C.V., Thomas, L.E., Adamson, K.R., 2010. Pleistocene ice caps on the coastal mountains of the Adriatic Sea. Quat. Sci. Rev. 29, 3690–3708.
Jablonski, N.G., Whitfort, M.J., Roberts-Smith, N., Xu, Q.Q., 2000. The influence of life history and diet on the distribution of catarrhine primates during the Pleistocene in eastern Asia. J. Hum. Evol. 39, 131–157.
Ji, H.X., 1975. The lower Pleistocene mammalian fossils of Lantian Distriet, Shensi. Vert PalAsiat 13 (3), 169–177 (in Chinese with English summary).
Kaiser, T.M., Müller, D.W., Fortelius, M., Schulz, E., Codron, D., Clauss, M., 2013. Hypsodonty and tooth facet development in relation to diet and habitat in herbivorous ungulates: implications for understanding tooth wear. Mammal Rev. 43 (1), 34–46.
Kauman, D.S., Manley, W.F., 2004. Pleistocene Maximum and Late Wisconsinan glacier extents across Alaska, U.S.A. Dev. Quat. Sci. 2, 9–27.
Lisiecki, L.E., Raymo, M.E., 2005. A Pliocene-Pleistocene stack of 57 globally distributed benthic $\delta^{18}O$ records. Paleoceanography 20, 1–16.
Lister, A.M., 2011. The impact of Quaternary Ice Ages on mammalian evolution. Philos. Trans. R. Soc., B 359, 221–241.
Liu, T., Ding, Z., 1993. Stepwise coupling of monsoon circulations to global ice volume variations during the late Cenozoic. Glob. Planet. Chang. 7, 119–130.
Marjanac, T., Marjanac, L., 2016. The extent of middle Pleistocene ice cap in the coastal Dinaric Mountains of Croatia. Quat. Res. 85, 445–455.
Museum of Liaoning Province, Museum of Benxi City, 1986. Miaohoushan-A Site of Early Paleolithic in Benxi County, Liaoning. Wenwu Press, Beijing, pp. 1–110 (in Chinese with English summary).
Norton, C.J., 2000. The current state of Korean paleoanthropology. J. Hum. Evol. 38, 803–825.
Norton, C.J., Jin, C.Z., Wang, Y., Zhang, Y.Q., 2010. Rethinking the Palearctic-Oriental biogeographic boundary in Quaternary China. In: Norton, C.J., Braun, D. (Eds.), Asian Paleoanthropology: From Africa to China and Beyond. Vertebrate Paleobiology and Paleoanthropology Series. Springer Press, Dordrecht, The Netherlands, pp. 81–100.
Polyak, L., Alley, R.B., Andrews, J.T., Brigham-Grette, J., Cronin, T.M., Darby, D.A., Dyke, A.S., Fitzpatrick, J.J., Funder, S., Holland, M., 2010. History of sea ice in the Arctic. Quat. Sci. Rev. 29, 1757–1778.
Potts, R., 2012. Evolution and environmental change in early human prehistory. Annu. Rev. Anthropol. 41, 151–167.
Qi, J., Yang, Q., 2010. Cenozoic structural deformation and dynamic processes of the Bohai Bay basin province, China. Mar. Pet. Geol. 27, 757–771.
Qiu, Z.X., 2006. Quaternary environmental changes and evolution of large mammals in North China. Vertebrata Palasiatica 44, 109–132.
Qiu, Z.X., Huang, W.L., Guo, Z.H., 1987. The Chinese hipparione fossils. Acta Palaeontol. Sin. New Ser. C (25), 1–250 (in Chinese with English sunmmary).
Shen, G., Gao, X., Gao, B., Granger, D.E., 2009. Age of Zhoukoudian Homo erectus determined with $^{26}Al/^{10}Be$ burial dating. Nature 458, 198–200.
Shipley, L.A., 1999. Grazers and Browsers: How Digestive Morphology Affects Diet Selection. Grazing Behavior of Livestock and Wildlife. 70. pp. 20–27.
Smith, F.A., Boyer, A.G., Brown, J.H., Costa, D.P., Dayan, T., Ernest, S.K.M., Evans, A.R., Fortelius, M., Gittleman, J.L., Hamilton, M.J., Harding, L.E., Lintulaakso, K., Lyons, S.K., McCain, C., Okie, J.G., Saarinen, J.J., Sibly, R.M., Stephens, P.R., Theodor, J., Uhen, M.D., 2010. The evolution of maximum body size of terrestrial mammals. Science 330, 1216–1219.
Teilhard de Chardin, P., 1940. The fossils from Locality 18 near Peking. Acta Palaeontol. Sin. New Ser. C 9, 1–94.
Teilhard de Chardin, P., Pei, W.C., 1941. The fossil mammals of Locality 13 in Choukoutien. Acta Palaeontol. Sin. New Ser. C 11, 1–106.
Wang, P., Tian, J., Cheng, X., Liu, C., Xu, J., 2003. Carbon reservoir changes preceded major ice-sheet expansion at the mid-Brunhes event. Geology 31, 239–242.
Wei, G.B., 2004. Taxonomy and Biostratigraphy of the Middle Pliocene–Early Pleistocene Mammuthus of Northem China, With Discussion on the Evolution of Eurasian Mammoths. City Univ, Dr Dissert, Osaka, pp. 1–112.
White, J.W.C., Alley, R.B., Brigham-Grette, J., Fitzpatrick, J.J., Jennings, A.E., Johnsen, S.J., Miller, G.H., Nerem, R.S., Polyak, L., 2010. Past rates of climate change in the Arctic. Quat. Sci. Rev. 29, 1716–1727.
Wu, F., Fang, X., Ma, Y., Herrmann, M., Mosbrugger, V., An, Z., Miao, Y., 2007. Plio–Quaternary stepwise drying of Asia: evidence from a 3-Ma pollen record from the Chinese Loess Plateau. Earth Planet. Sci. Lett. 257, 160–169.
Wu, R.K., Wu, X.Z., Zhang, S.S., 1989. Early Humankind in China. Science Press, Beijing, pp. 1–437 (in Chinese).
Xiao, G.Q., Yang, J.L., Zhao, C.R., Wang, Q., Xu, Q.M., Hu, Y.Z., Qin, Y.F., Li, J., Xiao, G.Q., 2014. Magnetostratigraphy of drill hole G2 in the Tianjin coastal area and its tectonic significance. Geol. Bull. China 33 (10), 1642–1650 (in Chinese with English summary).
Yang, D., Fang, X.M., Dong, G.R., Peng, Z.C., Li, J.J., 2006. Aeolian deposit evidence for formation and evolution of the Tengger Desert in the north of China since early Pleistocene. Mar. Geol. Quat. Geol. 26, 93–100 (in Chinese with English summary).
Yang, J.L., Xu, Q.M., Hu, Y.Z., Yuan, H.F., Xiao, G.Q., Zhou, X.Y., 2016. Palaeovegetation evolution and its response to the climate change since Middle Pleistocene in the North China Plain. Geol. Bull. China 35 (10), 1745–1751 (in Chinese with English summary).
Yi, L., Deng, C., Tian, L., Xu, X., Jiang, X., Qiang, X., Qin, H., Ge, J., Chen, G., Su, Q., 2016. Plio-Pleistocene evolution of Bohai Basin (East Asia): demise of Bohai Paleolake and transition to marine environment. Sci. Rep. 6, 29403.
Zhang, S.S., 1993. Comprehensive study of the Jinniushan paleolithic site. Mem IVPP AS 19, 1–163 (in Chinese with English summary).
Zubakov, V.A., Borenkova, I.I., 1990. Global Palaeoclimate of the Late Cenozoic. Elsevier.